



This is a repository copy of *Bimetallic Pt(II)-bipyridyl-diacetylde/Ln(III) tris-diketonate adducts based on a combination of coordinate bonding and hydrogen bonding between the metal fragments: syntheses, structures and photophysical properties* .

White Rose Research Online URL for this paper:
<http://eprints.whiterose.ac.uk/7970/>

Article:

Al-Rasbi, N.K., Derossi, S., Sykes, D. et al. (2 more authors) (2009) Bimetallic Pt(II)-bipyridyl-diacetylde/Ln(III) tris-diketonate adducts based on a combination of coordinate bonding and hydrogen bonding between the metal fragments: syntheses, structures and photophysical properties. *Polyhedron*, 28 (2). pp. 227-232. ISSN 0277-5387

<https://doi.org/10.1016/j.poly.2008.10.046>

Reuse

Unless indicated otherwise, fulltext items are protected by copyright with all rights reserved. The copyright exception in section 29 of the Copyright, Designs and Patents Act 1988 allows the making of a single copy solely for the purpose of non-commercial research or private study within the limits of fair dealing. The publisher or other rights-holder may allow further reproduction and re-use of this version - refer to the White Rose Research Online record for this item. Where records identify the publisher as the copyright holder, users can verify any specific terms of use on the publisher's website.

Takedown

If you consider content in White Rose Research Online to be in breach of UK law, please notify us by emailing eprints@whiterose.ac.uk including the URL of the record and the reason for the withdrawal request.



eprints@whiterose.ac.uk
<https://eprints.whiterose.ac.uk/>

promoting access to White Rose research papers



Universities of Leeds, Sheffield and York
<http://eprints.whiterose.ac.uk/>

This is an author produced version of a paper published in **Polyhedron**.

White Rose Research Online URL for this paper:

<http://eprints.whiterose.ac.uk/7970/>

Published paper

Al-Rasbi, N.K., Derossi, S., Sykes, D., Faulkner, S. and Ward, M.D. (2009)
Bimetallic Pt(II)-bipyridyl-diacetylde/Ln(III) tris-diketonate adducts based on a combination of coordinate bonding and hydrogen bonding between the metal fragments: syntheses, structures and photophysical properties. *Polyhedron*, 28 (2). pp. 227-232.

<http://dx.doi.org/10.1016/j.poly.2008.10.046>

Submitted by:

Prof. Michael D. Ward
Department of Chemistry
University of Sheffield
SHEFFIELD
S3 7HF
Tel: 0114 2229484
Fax: 0114 2229346

Bimetallic Pt(II)-bipyridyl-diacetylide / Ln(III) tris-diketonate adducts based on a combination of coordinate bonding and hydrogen bonding between the metal fragments; syntheses, structures and photophysical properties.

Nawal K. Al-Rasbi,^a Sofia Derossi,^a Daniel Sykes,^b Stephen Faulkner,^b and Michael D. Ward^{a*}

^a *Department of Chemistry, University of Sheffield, Sheffield S3 7HF, UK*
Email: m.d.ward@sheffield.ac.uk

^b *Department of Chemistry, University of Manchester, Oxford Road, Manchester M13 9PL, UK*

Abstract

The luminescent Pt(II) complex $[\text{Pt}(4,4'\text{-}^t\text{Bu}_2\text{-bipy})\{\text{CC}-(5\text{-pyrimidinyl})\}_2]$ (**1**) was prepared by coupling of $[\text{Pt}(4,4'\text{-}^t\text{Bu}_2\text{-bipy})\text{Cl}_2]$ with 5-ethynyl-pyrimidine, and contains two pyrimidinyl units pendant from a Pt(II) bipyridyl diacetylide core; it shows luminescence at 520 nm which is typical of Pt(II) luminophores of this type. Reaction with $[\text{Ln}(\text{hfac})_3(\text{H}_2\text{O})_2]$ (hfac = anion of hexafluoroacetylacetone) affords as crystalline solids the compounds $[\mathbf{1} \cdot \{\text{Ln}(\text{hfac})_3(\text{H}_2\text{O})\} \{\text{Ln}(\text{hfac})_3(\text{H}_2\text{O})_2\}]$ (Ln = Nd, Gd, Er, Yb), in which the $\{\text{Ln}(\text{hfac})_3(\text{H}_2\text{O})\}$ unit is coordinated to one pyrimidine ring *via* an N atom, whereas the $\{\text{Ln}(\text{hfac})_3(\text{H}_2\text{O})_2\}$ unit is associated with two N atoms, one from each pyrimidine ring of **1**, *via* N...HOH hydrogen-bonding interactions involving the coordinated water ligands on the lanthanide centre. Solution spectroscopic studies show that the luminescence of **1** is partly quenched on addition of $[\text{Ln}(\text{hfac})_3(\text{H}_2\text{O})_2]$ (Ln = Er, Nd) by formation of Pt(II)/Ln(III) adducts in which Pt(II)→Ln(III) photoinduced energy-transfer occurs to the low-lying f-f levels of the Ln(III) centre. Significant quenching occurs with both Er(III) and Nd(III) because both have several f-f states which match well the ³MLCT emission energy of **1**. Time-resolved luminescence studies show that Pt(II)→Er(III) energy-transfer ($7.0 \times 10^7 \text{ M}^{-1}$) is around three times faster than Pt(II)→Nd(III) energy-transfer ($\approx 2 \times 10^7 \text{ M}^{-1}$) over the same distance because the luminescence spectrum of **1** overlaps better with the absorption spectrum of Er(III) than with Nd(III). In contrast Yb(III) causes no significant quenching of **1** because it has only a single f-f excited level which is a poor energy match for the Pt(II)-based excited state.

Introduction

There has been extensive recent interest in the preparation and photophysical properties of d-f dinuclear complexes in which d-block chromophores, generally with long-lived MLCT excited states, are used as energy-donors to generate sensitised near-infrared luminescence from lanthanide(III) ions such as Nd(III) and Yb(III) which have low-lying emissive f-f states [1-4]. The intense and fully allowed ¹MLCT absorptions of the d-block unit allow light to be absorbed at a range of wavelengths in the visible region, overcoming the inability of lanthanide(III) ions to absorb light themselves due to the f-f transitions being Laporte-forbidden. Two recent results of particular significance are (i) that d→f energy-transfer occurs by the Dexter mechanism over long distances (up to 20 Å) when conjugated bridging ligands are used to link the d-block and f-block components [3], and (ii) there is a clear correlation of energy-transfer rate with donor/acceptor spectroscopic overlap [4], which is to be expected but was nonetheless clearly demonstrated in some Pt(II)/Ln(III) dyads in which the ³MLCT energy of the Pt(II) unit varied [4].

In this paper we report a new series of Pt(II)/Ln(III) dyads based on a luminescent Pt(II)-diimine-diacetylide chromophore [4,5] which bears two pendant pyrimidinyl groups. These groups in turn provide four N-donor sites which could potentially act as sites of attachment to {Ln(diketonate)₃} centres to allow buildup of polynuclear Pt(II)/Ln(III) assemblies. We describe the synthesis and structure of the new Pt(II) unit, the unexpected structure of a trinuclear PtEr₂ adduct, and the photophysical properties of some 1:1 Pt/Ln assemblies (Ln = Gd, Er, Nd, Yb) in solution, in which Pt→Ln energy-transfer occurs to varying extents depending on the nature of the Ln(III) centres.

Results and Discussion

The new Pt(II) complex **1** (Scheme 1) was prepared from the Cu(I)-catalysed coupling of 4-ethynylpyrimidine with [Pt(^tBu₂bipy)Cl₂] according to the literature method [5], followed by chromatographic purification to give pure **1** in 64% yield. Satisfactory spectroscopic and analytical data were obtained (see Experimental section). X-ray quality crystals were grown by slow evaporation of a CH₂Cl₂ solution of **1**; the crystal structure is shown in Figure 1. The Pt(II) ion is in the usual square planar coordination environment, with the Pt-N(py) bond lengths being significantly longer than the Pt-C bond lengths, as is typical for complexes of this type. One pyrimidine ring [containing N(32) and N(34)] is twisted out of the plane of the

^tBu₂bipy ligand by 30°; this deviation of a ring from overall planarity prevents the molecules from forming well-defined columnar stacks. Stacking between adjacent molecules involves the {Pt(bipy)} cores, separated by (on average) 3.4 Å and is shown in Fig. 1(b); there are no short Pt•••Pt contacts.

The UV/Vis absorption spectrum of **1** in CH₂Cl₂ shows absorption maxima at 378 nm (ϵ , 8.7 x 10³ M⁻¹ cm⁻¹) and 287 nm (ϵ , 44 x 10³ M⁻¹ cm⁻¹) which can be assigned to ¹MLCT and ligand-centred π - π^* transitions respectively. Excitation of the complex into the ¹MLCT absorption band generates typical strong luminescence at 520 nm with τ = 105 ns and ϕ = 3.7% (in air-equilibrated CH₂Cl₂) which may be ascribed to a ³MLCT process [4,5]. Thus, the complex has the potential to act as an energy-donor to Ln(III) ions whose f-f states are lower in energy than the ³MLCT energy of **1** [1-4].

Reaction of **1** with [Ln(hfac)₃(H₂O)₂] (Ln = Gd, Nd, Er, Yb) in CH₂Cl₂ solution, followed by layering heptane on to the reaction mixture and leaving the solutions to stand for several days, afforded reasonable yields of orange crystalline products for which elemental analysis was consistent with a 1:2 association of Pt(II) complex **1** and {Ln(diketonate)₃} units, respectively. This reaction exploits the lability of the two water ligands of [Ln(hfac)₃(H₂O)₂] units and their tendency to be replaced by N-heterocyclic donors [1-4]. We had expected that the pyrimidine rings might act as bridging ligands, each spanning two Ln(III) centres to generate network structures. However the crystal structure of [**1**•{Er(hfac)₃(H₂O)}]{Er(hfac)₃(H₂O)₂} (Figs. 2, 3) reveals a trinuclear PtEr₂ species in which the {Er(hfac)₃} units interact with the pyrimidine rings of **1** by a combination of conventional N—Er dative bonds, and N•••HOH hydrogen bonds to the water molecules that are in turn coordinated to the Er(III) centres. Thus Er(1) is 8-coordinate from three diketonate ligands, one water ligand, and one directly coordinated pyrimidine N atom [N(4)]. Er(2) is also 8-coordinate, from three diketonate and two water ligands, and is associated with both pyrimidine rings of **1** by a pair of N•••HOH hydrogen bonding interactions: effectively complex **1** behaves as a chelating bidentate H-bond acceptor to this {Er(hfac)₃(H₂O)₂} unit. The non-bonded N•••O distances in these hydrogen-bonds are N(2)•••O(2W), 2.764(7) Å and N(12)•••O(3W), 2.770(7) Å. The N•••H—O angles are 168.8 and 161.8° respectively. The arrangement of this pair of pyrimidine N atoms [N(2) and N(12)], both oriented inwards towards the same cavity, makes an ideal hydrogen-bond accepting site for the {Er(hfac)₃(H₂O)₂} unit. We have seen a similar hydrogen-bonding interaction between a coordinated water ligand and a weakly basic N-heterocyclic donor, in which the heterocycle does not coordinate directly to the Ln(III) centre, in previous work [6].

The geometry around both Er(III) centres is approximately square antiprismatic, as shown in Fig. 3 which emphasises their immediate coordination environments. For Er(1) the two square planes consist of O(1)/O(3)/O(4)/N(4) and O(2)/O(5)/O(6)/O(1W); for Er(2) the two planes consist of O(8)/O(10)/O(3W)/O(2W) and O(7)/O(9)/O(11)/O(12). The two Er(III) units are 8.99 Å apart; the Pt•••Er separations are 8.67 Å to Er(1) and 8.81 Å to Er(2). The tendency we see in this complex of the pyrimidine N atoms not to coordinate fully to the Ln(III) centres presumably reflects the poorer basicity of pyrimidine compared to pyridine.

Spectroscopic titrations were then performed in which small portions of [Ln(hfac)₃(H₂O)₂] were added to a solution of **1** (5 x 10⁻⁵ M) in CH₂Cl₂. This addition resulted in no perceptible change to the position or intensity of the ¹MLCT absorption band at 378 nm, but resulted in significant changes in luminescence intensity depending on the nature of Ln(III). The decrease in luminescence during the titration when Ln = Er is shown in Fig. 4. During this titration the luminescence intensity from **1** was slightly blue-shifted from 520 to 510 nm, and steadily diminished in intensity. The blue-shift is consistent with the energy of the ³MLCT state being increased by the coordinated Er(III) centre attached to a pyrimidine ring (*cf.* the crystal structure). This arises because of the electron-withdrawing effect of the electropositive Er(III) ion, which inductively stabilises the Pt(II) d(π) orbitals and slightly increases the Pt(II)→bipy MLCT energy gap [4]. The steady reduction in luminescence intensity during the titration, on the other hand, must arise from Pt(II)→Er(III) energy-transfer which quenches the Pt(II)-based excited state by generation of an f-f excited state at Er(III).

A plot of decrease in luminescence intensity of **1** vs. amount of added [Er(hfac)₃(H₂O)₂] produced a curve which fitted well to a 1:1 binding isotherm, from which an association constant of 7 x 10³ M⁻¹ could be calculated. We do not know what the solution structure of the adduct (denoted **1**•Er) is: it may differ significantly from what was observed in the solid state (a kinetic species) although adduct formation is clearly occurring. The most likely behaviour – based on extensive previous work [4,7] – is that an {Er(hfac)₃} fragment is bound to **1** *via* one of the weakly basic pendant pyrimidine N atoms, *cf.* atom Er(1) in Fig. 2. An association constant of 7 x 10³ M⁻¹ involving binding of an {Er(hfac)₃} fragment to a single pyrimidine ring is reasonable given that we have obtained association constants of the order of 10⁵ M⁻¹ for binding to a chelating 2,2'-bipyrimidine site in a neutral complex [7b]. We could not find any evidence for a 1:2 Pt:Er adduct (*cf.* the crystal structure) in which a second {Ln(hfac)₃} fragment is associated *via* hydrogen-bonding. Presumably the second

association constant is too low to have any noticeable effect at the low concentrations used for photophysical studies.

As a control experiment we performed the same titration of **1** with [Gd(hfac)₃(H₂O)₂]. Gd(III) cannot quench the excited state of **1** because its lowest energy f-f excited state is at 32000 cm⁻¹, in the UV region. Thus Gd(III) behaves the same as other Ln(III) ion terms of electrostatic and steric effects, but without being able to cause quenching by energy-transfer. In this experiment, addition of portions of [Gd(hfac)₃(H₂O)₂] to a solution of **1** resulted in a slight *increase* in emission intensity – consistent with the increase in energy of the ³MLCT state – and a corresponding increase in emission lifetime to 141 ns. This lifetime of 141 ns for the adduct between **1** and {Gd(hfac)₃} is then used as the basis for comparison with other **1**•Ln₂ adducts in solution.

$$k_{\text{EnT}} = 1/\tau_1 - 1/\tau_2 \quad (1)$$

At the end of the titration of **1** with [Er(hfac)₃(H₂O)₂], the partially-quenched Pt(II)-based emission of **1** displayed dual-exponential decay with lifetimes of 96 ns (major component) and 13 ns (minor component). Given that the titration did not go to completion, because of the relatively low association constant of 7 x 10³ M⁻¹, we assign the 96 ns component to luminescence from free **1** which was measured as 105 ns in the absence of any added [Er(hfac)₃(H₂O)₂] (the slight reduction from 105 ns to 96 ns may be ascribed to collisional quenching between **1** and increasing amounts of [Er(hfac)₃(H₂O)₂] even when adduct formation is not occurring). The 13 ns component may be ascribed to nearly-quenched emission from the Pt(II) centre in the adduct **1**•Er. From eq. 1 [in which k_{EnT} is the energy-transfer rate, and τ_1 (13 ns) and τ_2 (141 ns) are the partially-quenched and unquenched Pt(II)-based luminescence lifetimes respectively], we can determine the Pt(II)→Er(III) energy-transfer rate to be 7.0 x 10⁷ sec⁻¹.

An exactly similar experiment with [Yb(hfac)₃(H₂O)₂] resulted in no significant quenching, with **1**•Yb₂ showing essentially identical properties to **1**•Gd₂ with a final lifetime of 137 ns. Application of eq. 1 gives $k_{\text{EnT}} \approx 2 \times 10^5 \text{ sec}^{-1}$, although given the very small difference between the values of τ_1 (137 ns) and τ_2 (141 ns), each individually having a margin of error of at least 2%, this calculation is of little significance and we can just say that there is essentially no Pt(II)→Yb(III) energy-transfer.

When $[\text{Nd}(\text{hfac})_3(\text{H}_2\text{O})_2]$ was used in the titration, the luminescence from **1** was again steadily, but not completely, quenched. At the end of the titration – after addition of 10 equivalents of $[\text{Nd}(\text{hfac})_3(\text{H}_2\text{O})_2]$ – the decay curve showed signs of dual exponential decay, although it this was difficult to deconvolute into two components with confidence. If we fixed one component at 105 ns, being unchanged luminescence from the substantial amount of free **1**, the second component refined to being *ca.* 30 – 40 ns from several independent measurements. If we take an estimate of 35 ns for the partially-quenched luminescence of **1**•Nd we get from eq. 1 a Pt(II)→Nd(III) energy-transfer rate constant of *ca.* $2 \times 10^7 \text{ sec}^{-1}$, about one-third the value of the value Pt(II)→Er(III) energy-transfer rate constant ($7.0 \times 10^7 \text{ sec}^{-1}$).

The ability of these different lanthanide(III) ions to accept energy from the $^3\text{MLCT}$ state of **1** is therefore in the order $\text{Er} > \text{Nd} > \text{Yb}$, which agrees with what we have seen before in Pt(II)/Ln(III) dyads where the Pt(II) emission is quite high in energy [4]. The results can be rationalised on the basis of overlap between the donor's emission spectrum and the acceptor's absorption spectrum. Yb(III) only has a single f-f absorption at $10,200 \text{ cm}^{-1}$ which has negligible overlap with the tail end of the luminescence spectrum of **1**. Nd(III) is much richer in f-f excited states in the relevant region (Fig. 5, 6), with ten f-f levels lying between 11000 and 20000 cm^{-1} (910 and 500 nm) spanning the region where the Pt-based emission occurs; however, the Nd(III)-based f-f absorptions are weak in the area where the Pt(II) emission is at its most intense (Fig. 6). In contrast, the region of maximum f-f absorption intensity for Er(III) – between 520 and 530 nm (Fig. 6) – exactly matches the emission maximum of **1**, giving good donor/acceptor overlap which results in Er(III) being the best energy acceptor from complex **1** from this set of Ln(III) ions.

We note also that the absolute values of these energy-transfer rates are slower than we observed before in other Pt(II)-Ln(III) dyads [4], despite the inter-metallic distances being shorter. This is likely to be a consequence of the bridging pathway which provides the necessary electronic coupling for Dexter energy-transfer [3]. In the crystal structure of **1**•Er₂ we can see that one $\{\text{Er}(\text{hfac})_3\}$ unit is only connected to **1** *via* hydrogen-bonding, through which electronic coupling will necessarily be weak, and the other is connected to the N atoms of a pyrimidine ring which has a *meta* relationship to the acetylide 'wire'. The relative weakness of electronic couplings across *meta*-substituted aromatic rings compared to *para* linkages is well known [8].

Even though it is relatively slow, Pt(II)→Ln(III) energy-transfer is clearly occurring to Nd(III) and Er(III). We attempted therefore to see if we could see sensitised Ln(III)-based

emission from these centres following excitation of the MLCT absorption of **1** at 450 nm. We could not detect any significant sensitised Nd(III)-based or Er(III)-based luminescence under these conditions however, which is likely to be a consequence of (i) slow energy-transfer leading to only a fraction of the Ln(III) centres being excited by this mechanism, (ii) the relatively low absorbance of the adducts at 450 nm, and (iii) the presence of water molecules in the coordination spheres of these ions (according to the crystal structure) which will make any luminescence weak and short-lived. It is well known that directly coordinated OH oscillators are very effective at quenching low-energy luminescence from lanthanide(III) ions [9].

We could however detect weak Nd(III)-based emission using 337 nm excitation which directly excites the Ln(III) centres *via* the diketonate π - π^* absorptions in a region where the extinction coefficient is much higher, and in this case we could detect weak luminescence from Nd(III) at its characteristic wavelengths of 1060 and 1340 nm; this emission clearly showed dual-exponential decay with lifetimes of *ca.* 1.0 and 0.2 μ s, in agreement with the presence of two environments for Nd(III), one with two coordinated water molecules (to which can be ascribed the shorter-lived lifetime component) [4] and the other with only one coordinated water molecule (to which can be ascribed the longer-lived lifetime component). Similarly, direct excitation of the $\{\text{Er}(\text{hfac})_3\}$ centre in **1**•Er₂ using 337 nm excitation revealed very weak luminescence at 1530 nm characteristic of Er(III) (too weak for lifetime measurements to be reliable, due to the coordinated water ligands).

In conclusion, the new luminescent complex **1**, with two pendant pyrimidinyl units, forms adducts with $\{\text{Er}(\text{hfac})_3(\text{H}_2\text{O})_n\}$ fragments ($n = 1, 2$) which in the solid state are associated by a combination of direct Pt—Er dative bonds, and N•••HOH hydrogen bonds between pyrimidine rings and the water molecules coordinated to Er(III). This association results in Pt→Ln photoinduced energy-transfer to lanthanide(III) ions having low-lying f-f states, with energy transfer rates in the order Pt→Er > Pt→Nd > Pt→Yb, in agreement with expectations based on the availability of f-f states on these lanthanide ions which can act as energy-acceptors and how well they overlap with the luminescence from **1**. The presence of coordinated water molecules still attached to the Ln(III) centres however means that the resulting sensitised near-infrared luminescence is very weak.

Experimental

General details

The following were prepared using literature methods: $[\text{Ln}(\text{hfac})_3(\text{H}_2\text{O})_2]$ [10], $[\text{Pt}(\text{}^t\text{Bu}_2\text{bipy})\text{Cl}_2]$ [4]. The following instruments were used for routine spectroscopic measurements: UV/Vis spectra, and Cary 50 spectrophotometer; luminescence spectra, a Perkin-Elmer LS-50 fluorimeter; luminescence lifetimes in the visible region, an Edinburgh Instruments 'mini- τ ' time-resolved fluorimeter equipped with a 405 nm pulsed diode laser excitation source; EI mass spectra, a VG AutoSpec magnetic sector instrument; ^1H NMR spectra, a Bruker AC-250 spectrometer. Lanthanide-based luminescence lifetimes in the near-infrared region were measured using a setup described previously [11].

X-ray crystallography

X-ray crystallographic data are summarised in Table 1. For each compound a suitable crystal was coated with hydrocarbon oil and attached to the tip of a glass fibre and transferred to a Bruker-SMART 1000 or APEX-2 CCD diffractometer (graphite-monochromated Mo-K α radiation, $\lambda = 0.71073 \text{ \AA}$) under a stream of cold N_2 . Data were corrected for Lorentz and polarisation effects and for absorption by semi-empirical methods (SADABS) [12] based on symmetry-equivalent and repeated reflections. The structures were solved by direct methods or heavy atom Patterson methods and refined by full-matrix least-squares methods on F^2 . Hydrogen atoms were placed geometrically and refined with a riding model and with U_{iso} constrained to be 1.2 (1.5 for methyl groups) times U_{eq} of the carrier atom. Structures were solved and refined using the SHELX suite of programs [13]. Significant bond distances and angles for the structures of the metal complexes are in Tables 2 and 3. The structure determination of **1** presented no significant problems. In $[\mathbf{1} \cdot \{\text{Er}(\text{hfac})_3(\text{H}_2\text{O})_2\} \{\text{Er}(\text{hfac})_3(\text{H}_2\text{O})\}]$ however there was rotational disorder involving both some of the CF_3 groups of the hfac ligand, and some of the ${}^t\text{Bu}$ groups of the ${}^t\text{Bu}_2\text{bipy}$ ligands. Specifically the CF_3 groups involving C atoms C(55), C(61), C(65) and C(85) exhibited disorder of the attached F atoms, with two or three F atoms at each of these CF_3 groups disordered over two positions with site occupancies of 51% and 49%. Likewise the methyl groups C(38) and C(39) were disordered over two sites each with the same fractional occupancies. These disordered atoms, with fractional site occupancies, were refined with isotropic displacement parameters.

Supplementary data (cif files for the two structures) are available on request from the Cambridge Crystallographic Data Centre, 12 Union Road, Cambridge, CB2 1EZ, UK, quoting deposition numbers 694403 and 694404 (see <http://www.ccdc.cam.ac.uk>).

Preparation of 5-ethynylpyrimidine. This is based on a literature method [14] but with some modifications. To a mixture of 5-bromopyrimidine (5.03 g, 31.6 mmol), Pd(PPh₃)₂Cl₂ (150 mg) and CuI (25 mg) in THF (15 mL) under N₂, was added 2-methyl-3-butyn-2-ol (2.60 g, 31.0 mmol) and diethylamine (30 mL). After stirring for 5 hrs at room temperature, the solvent was evaporated to dryness. Recrystallization from ethylacetate/diethylether afforded yellow microcrystalline needles of 2-methyl-4-(5-pyrimidine)-3-butyn-2-ol in 84.2 % yield. EI-MS: *m/z* 162 [*M*⁺]. ¹H NMR (250 MHz, CDCl₃): δ 9.10 (s, 1H; pyrimidine H²), 8.75 (d, 2H; pyrimidine H⁴/H⁶), 1.60 (s, 6H; 2CH₃): the OH peak could not be observed.

To a solution of 2-methyl-4-(5-pyrimidine)-3-butyn-2-ol (3.50 g, 33.7 mmol) in a mixture of toluene (30 mL) and diethylether (15 mL), was added finely powdered NaOH (0.80 g, 20 mmol). The mixture was refluxed for 3 hrs and was then cooled to room temperature and filtered. The solvent was concentrated in vacuum to 10 mL and cooled in the fridge. Pale yellow microcrystalline needles were isolated in 80% yield. EI-MS: *m/z* 104 [*M*⁺]. ¹H NMR (250 MHz, CDCl₃): δ 9.15 (s, 1H; pyrimidine H²), 8.80 (s, 2H; pyrimidine H⁴/H⁶) and 3.40 (s, 1H; CH).

Preparation of complex 1. A mixture of [Pt(4,4'-Bu₂bipy)Cl₂] (0.63 g, 1.20 mmol), anhydrous CuI (175 mg, catalyst), and dry *i*Pr₂NH (30 mL) in dry, degassed dichloromethane (150 mL) under N₂ was stirred for 10 min, after which time 4-ethynylpyrimidine (0.63 g, a large excess) was added. The resulting suspension was stirred under N₂ at room temperature for 5 days whilst being protected from light. The solvent was evaporated and the solid residue was dried *in vacuo* to remove traces of *i*Pr₂NH. The product was purified by column chromatography (2% MeOH-CH₂Cl₂/alumina) to give 0.53 g (64%) of the desired product. EI-MS: *m/z* 669 [*M*⁺]. ¹H NMR (250 MHz, CDCl₃): δ (ppm) 9.50 (2H, d; bpy H⁶), 8.90 (2H, s; pym H²), 8.74 (4H, s; pym H^{4,6}), 7.96 (2H, d; bpy H³), 7.58 (2H, dd; bpy H⁵) and 1.41 (18H, s; C(CH₃)₃). Found: C, 53.3; H, 4.3; N, 12.2. PtC₃₀H₃₀N₆ requires C, 53.8; H, 4.5; N, 12.5%. X-ray quality crystals were grown by slow evaporation of a CH₂Cl₂ solution.

Preparation of trinuclear complexes [1•{Ln(hfac)₃(H₂O)₂} {Ln(hfac)₃(H₂O)}] (1•Ln₂).

A solution of complex **1** (50 mg, 0.07 mmol) in CH₂Cl₂ was added to a solution of the appropriate [Ln(hfac)₃(H₂O)₂] (2 equiv) in CH₂Cl₂ and the mixture was stirred overnight. A small layer of heptane was placed over the solution and the system left to evaporate slowly until orange needles of the desired compounds grew in a few days. The crystals were filtered off, washed with hexane and dried.

Data for [1•{Nd(hfac)₃(H₂O)₂} {Nd(hfac)₃(H₂O)}]. Yield: 50 %. Found: C, 32.2; H, 1.8; N, 3.8. C₆₀H₄₂N₆O₁₅ F₃₆PtNd₂ requires C, 32.0; H, 1.9; N, 3.7%.

Data for [1•{Er(hfac)₃(H₂O)₂} {Er(hfac)₃(H₂O)}]. Yield: 53 %. Found: C, 31.8; H, 1.9; N, 3.9. C₆₀H₄₂N₆O₁₅ F₃₆PtEr₂ requires C, 31.3; H, 1.8; N, 3.7%.

Data for [1•{Yb(hfac)₃(H₂O)₂} {Yb(hfac)₃(H₂O)}]. Yield: 44 %. Found: C, 31.3; H, 1.8; N, 3.7. C₆₀H₄₂N₆O₁₅ F₃₆PtYb₂ requires C, 31.2; H, 1.8; N, 3.6%.

Data for [1•{Gd(hfac)₃(H₂O)₂} {Gd(hfac)₃(H₂O)}]. Yield: 48 %. Found: C, 31.8; H, 1.9; N, 3.7. C₆₀H₄₂N₆O₁₅F₃₆PtGd₂ requires C, 31.6; H, 1.8; N, 3.7%.

Acknowledgements

We thank the Government of the Sultanate of Oman and EPSRC for financial support, and Mr. William S. Perry for assistance with the near-IR luminescence measurements.

Table 1. Crystallographic data for the two new structures.

Compound	1	[1 •{Er(hfac) ₃ (H ₂ O)} {Er(hfac) ₃ (H ₂ O) ₂ }]
Formula	C ₃₀ H ₃₀ N ₆ Pt	C ₆₀ H ₄₂ Er ₂ F ₃₆ N ₆ O ₁₅ Pt
Formula weight	669.69	2270.01
<i>T</i> (K)	100(2) K	100(2) K
Crystal system, space group	Monoclinic, <i>P2(1)/c</i>	Monoclinic, <i>P2(1)/n</i>
<i>a</i> (Å)	14.3009(10)	15.9945(14)
<i>b</i> (Å)	11.1471(7)	17.2734(14)
<i>c</i> (Å)	18.0535(12)	28.924(2)
β (°)	113.046(3)	97.966(4)
<i>V</i> (Å ³)	2648.3(3)	7914.0(11)
<i>Z</i>	4	4
<i>D</i> _{calc}	1.680	1.905
μ (mm ⁻¹)	5.329	3.476
Crystal size (mm)	0.15 x 0.09 x 0.06	0.16 x 0.07 x 0.04
Reflections collected	55334	121054
Independent reflections	6135 [R(int) = 0.0288]	18083 [R(int) = 0.0447]
Data / restraints / parameters	6135 / 0 / 334	18083 / 22 / 1072
Final R indices ^a	<i>R</i> ₁ = 0.0161 <i>wR</i> ₂ = 0.0355	<i>R</i> ₁ = 0.0358 <i>wR</i> ₂ = 0.0854
Largest diff. peak and hole (e.Å ⁻³)	0.953, -0.489	1.883 and -2.298

^a The value of *R*₁ is based on selected data with $I > 2\sigma(I)$; the value of *wR*₂ is based on all data.

Table 2. Selected bond distances (Å) and angles (°) for the structure of **1**

Pt(1)-C(38)	1.946(2)
Pt(1)-C(28)	1.947(2)
Pt(1)-N(1)	2.0528(17)
Pt(1)-N(11)	2.0610(18)
C(38)-Pt(1)-C(28)	87.52(9)
C(38)-Pt(1)-N(1)	175.49(8)
C(28)-Pt(1)-N(1)	96.95(8)
C(38)-Pt(1)-N(11)	97.15(8)
C(28)-Pt(1)-N(11)	175.33(8)
N(1)-Pt(1)-N(11)	78.38(7)

Table 3. Selected bond distances (Å) and angles (°) in the structure of $[\mathbf{1} \cdot \{\text{Er}(\text{hfac})_3(\text{H}_2\text{O})\} \{\text{Er}(\text{hfac})_3(\text{H}_2\text{O})_2\}]$

Er(1)-O(3)	2.281(4)	Er(2)-O(9)	2.286(3)
Er(1)-O(5)	2.311(3)	Er(2)-O(10)	2.307(4)
Er(1)-O(4)	2.320(3)	Er(2)-O(7)	2.311(4)
Er(1)-O(6)	2.326(3)	Er(2)-O(12)	2.325(3)
Er(1)-O(2)	2.342(3)	Er(2)-O(3W)	2.334(3)
Er(1)-O(1W)	2.343(3)	Er(2)-O(8)	2.343(4)
Er(1)-O(1)	2.365(3)	Er(2)-O(2W)	2.343(4)
Er(1)-N(4)	2.532(4)	Er(2)-O(11)	2.357(4)
Pt(1)-C(8)	1.951(5)	Pt(1)-N(21)	2.055(4)
Pt(1)-C(18)	1.959(5)	Pt(1)-N(31)	2.065(4)

C(8)-Pt(1)-C(18)	85.73(19)	C(8)-Pt(1)-N(31)	174.54(17)
C(8)-Pt(1)-N(21)	95.93(17)	C(18)-Pt(1)-N(31)	99.44(18)
C(18)-Pt(1)-N(21)	177.44(18)	N(21)-Pt(1)-N(31)	78.84(16)

References

- [1] M. D. Ward, *Coord. Chem. Rev.* 251 (2007) 1663.
- [2] (a) S. Torelli, D. Imbert, M. Cantuel, G. Bernardinelli, S. Delahaye, A. Hauser, J.-C. G. Bünzli, C. Piguet, *Chem. Eur. J.* 11 (2005) 3228.
(b) S. J. A. Pope, B. J. Coe, S. Faulkner, R. H. Laye, *Dalton Trans.* (2005) 1482.
(c) P. D. Beer, F. Szemes, P. Passaniti, M. Maestri, *Inorg. Chem.* 43 (2004) 3965.
(d) P. B. Glover, P. R. Ashton, L. J. Childs, A. Rodger, M. Kercher, R. M. Williams, L. De Cola, Z. Pikramenou, *J. Am. Chem. Soc.* 125 (2003) 9918.
(e) H.-B. Xu, L.-X. Shi, E. Ma, L.-Y. Zhang, Q.-H. Wei, Z.-N. Chen, *Chem. Commun.* (2006) 1601.
(f) M. Mehlstäubl, G. S. Kottas, S. Colella, L. De Cola, *Dalton Trans.* (2008) 2385.
(g) J. W. Stouwdam, M. Raudsepp, F. C. J. M. van Veggel, *Langmuir*, 21 (2005) 7003.
(h) S. I. Klink, H. Keizer, F. C. J. M. van Veggel, *Angew. Chem. Int. Ed.* 39 (2000) 4319.
- [3] T. Lazarides, D. Sykes, S. Faulkner, A. Barbieri, M. D. Ward, *Chem. Eur. J.* 14 (2008) 9389.
- [4] T. K. Ronson, T. Lazarides, H. Adams, S. J. A. Pope, D. Sykes, S. Faulkner, S. J. Coles, M. B. Hursthouse, W. Clegg, R. W. Harrington, M. D. Ward, *Chem. Eur. J.* 12 (2006) 9299.
- [5] (a) S. L. James, M. Younus, P. R. Raithby, J. Lewis, *J. Organometal. Chem.* 542 (1997) 233.
(b) E. C. Whittle, J. A. Weinstein, M. W. George, K. S. Schanze, *Inorg. Chem.* 40 (2001) 4053.
(c) M. Hissler, M. Connick, D. K. Geiger, J. E. McGarrah, D. Lipa, R. J. Lachiotte, R. Eisenberg, *Inorg. Chem.* 39 (2000) 447.
- [6] Z. R. Reeves, K. L. V. Mann, J. C. Jeffery, J. A. McCleverty, M. D. Ward, F. Barigelletti, N. Armaroli, *J. Chem. Soc., Dalton Trans.* (1999) 349.
- [7] (a) T. Lazarides, H. Adams, D. Sykes, S. Faulkner, G. Calogero, M. D. Ward, *Dalton Trans.* (2008) 691.
(b) N. M. Shavaleev, G. Accorsi, D. Virgili, Z. R. Bell, T. Lazarides, G. Calogero, N. Armaroli and M. D. Ward, *Inorg. Chem.* 44 (2005) 61.
- [8] (a) J. A. McCleverty, M. D. Ward, *Acc. Chem. Res.* 31 (1998) 842.
(b) M. D. Ward, *Chem. Soc. Rev.* 24 (1995) 121.

- [9] (a) A. Beeby and S. Faulkner, *Chem. Phys. Lett.* 266 (1997) 116.
(b) A. Beeby, I. M. Clarkson, R. S. Dickins, S. Faulkner, D. Parker, L. Royle, A. S. de Sousa, J. A. G. Williams, M. Woods, *J. Chem. Soc. Perkin Trans 2*, (1999) 493.
- [10] Y. Hasegawa, Y. Kimura, K. Murakoshi, Y. Wada, J. Kim, N. Nakashima, T. Yamanaka, S. Yanagida, *J. Phys. Chem.* 100 (1996) 10201.
- [11] N. M. Shavaleev, S. J. A. Pope, Z. R. Bell, S. Faulkner, M. D. Ward, *Dalton Trans.* (2003) 808.
- [12] G. M. Sheldrick, *SADABS* version 2.10; University of Göttingen (2003).
- [13] G. M. Sheldrick, *SHELXS-97* and *SHELXL-97*; University of Göttingen (1997).
- [14] L. Yu, J. S. Lindsey, *J. Org. Chem.* 66 (2001) 7402.

Captions for Figures

- Fig. 1** (a) An ORTEP view of a molecule of complex **1**, with thermal ellipsoids at the 30% level; (b) a view showing stacking of adjacent molecules into pairs. H atoms are not shown for clarity.
- Fig. 2** An ORTEP view of a molecule of $[\mathbf{1} \cdot \{\text{Er}(\text{hfac})_3(\text{H}_2\text{O})\} \{\text{Er}(\text{hfac})_3(\text{H}_2\text{O})_2\}]$, with thermal ellipsoids at the 30% level. The dashed lines are hydrogen bonds between pyrimidine N atoms and water molecules coordinated to Er(2). H atoms (apart from those on the water ligands), F atoms on the hfac ligands, and the minor disorder component of the methyl groups on the ^tBu substituents, are not shown for clarity.
- Fig. 3** Coordination environments around (a) Er(1) and (b) Er(2) in the structure of $[\mathbf{1} \cdot \{\text{Er}(\text{hfac})_3(\text{H}_2\text{O})\} \{\text{Er}(\text{hfac})_3(\text{H}_2\text{O})_2\}]$. The dashed lines are hydrogen bonds between pyrimidine N atoms and water molecules coordinated to Er(2).
- Fig. 4** Steady decrease in the luminescence intensity of **1** (0.6 μM solution in CH₂Cl₂) as portions of $[\{\text{Er}(\text{hfac})_3(\text{H}_2\text{O})_2\}]$ (up to 9 equivalents) are added. Excitation was at 345 nm, a wavelength at which the absorbance of the solution did not change significantly during the titration.
- Fig. 5** Excited f-f levels of Nd(III), Er(III) and Yb(III).
- Fig. 6** Absorption spectra of $[\text{Ln}(\text{hfac})_3(\text{phen})]$ in CH₂Cl₂ (Ln = Nd, Er). Note the exact correspondence of the strong Er(III)-based absorption maximum in the 520 – 530 nm region with the ³MLCT emission maximum of **1** at 520 nm.

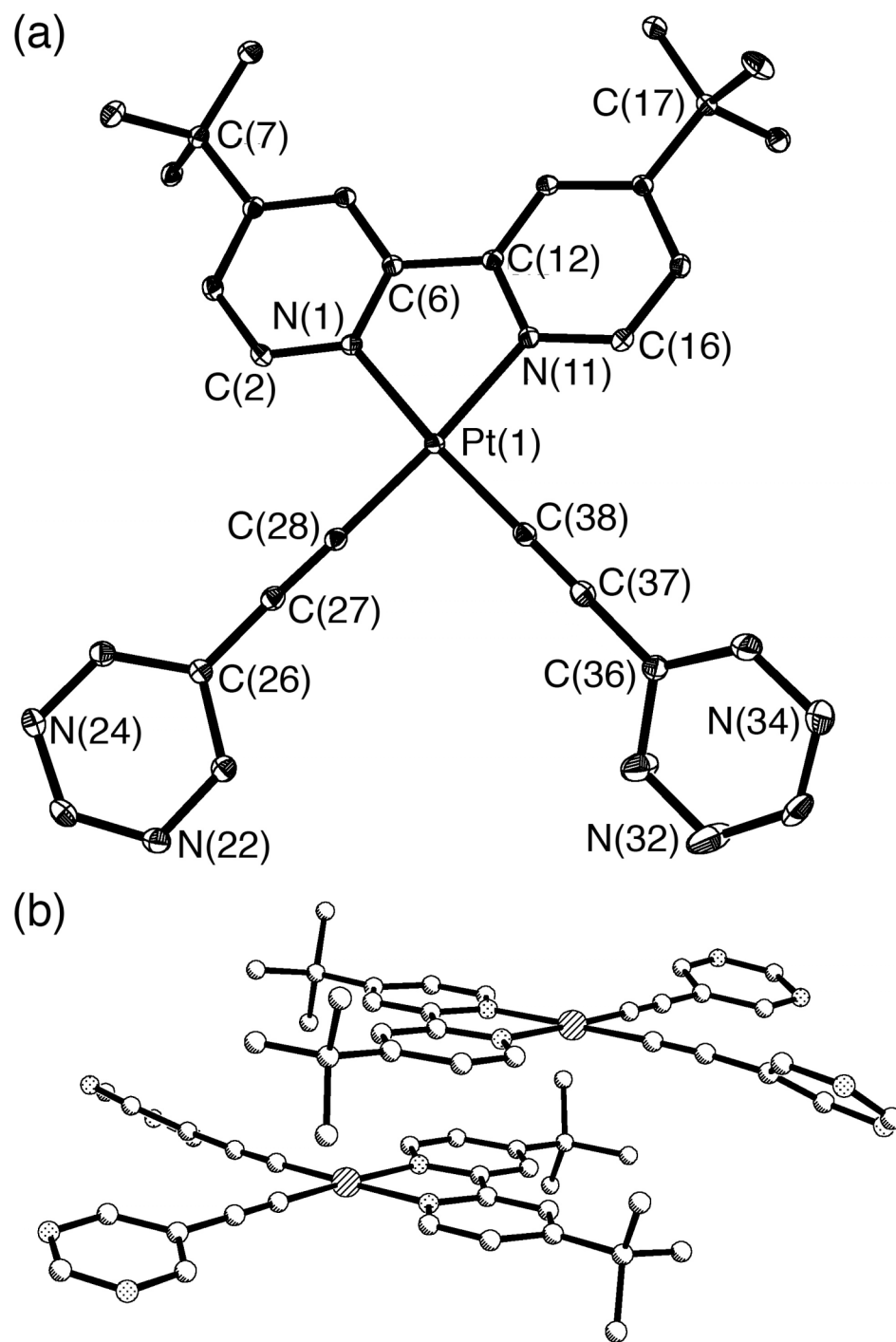


Figure 1

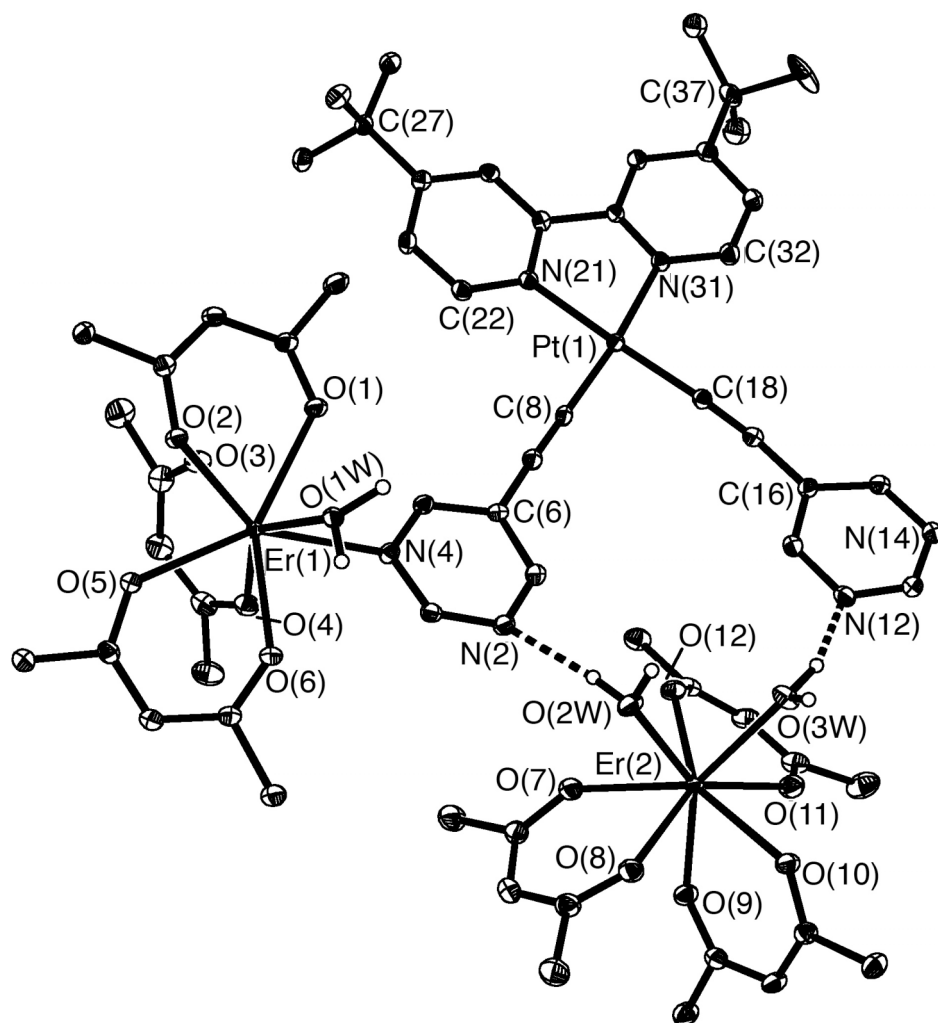


Figure 2

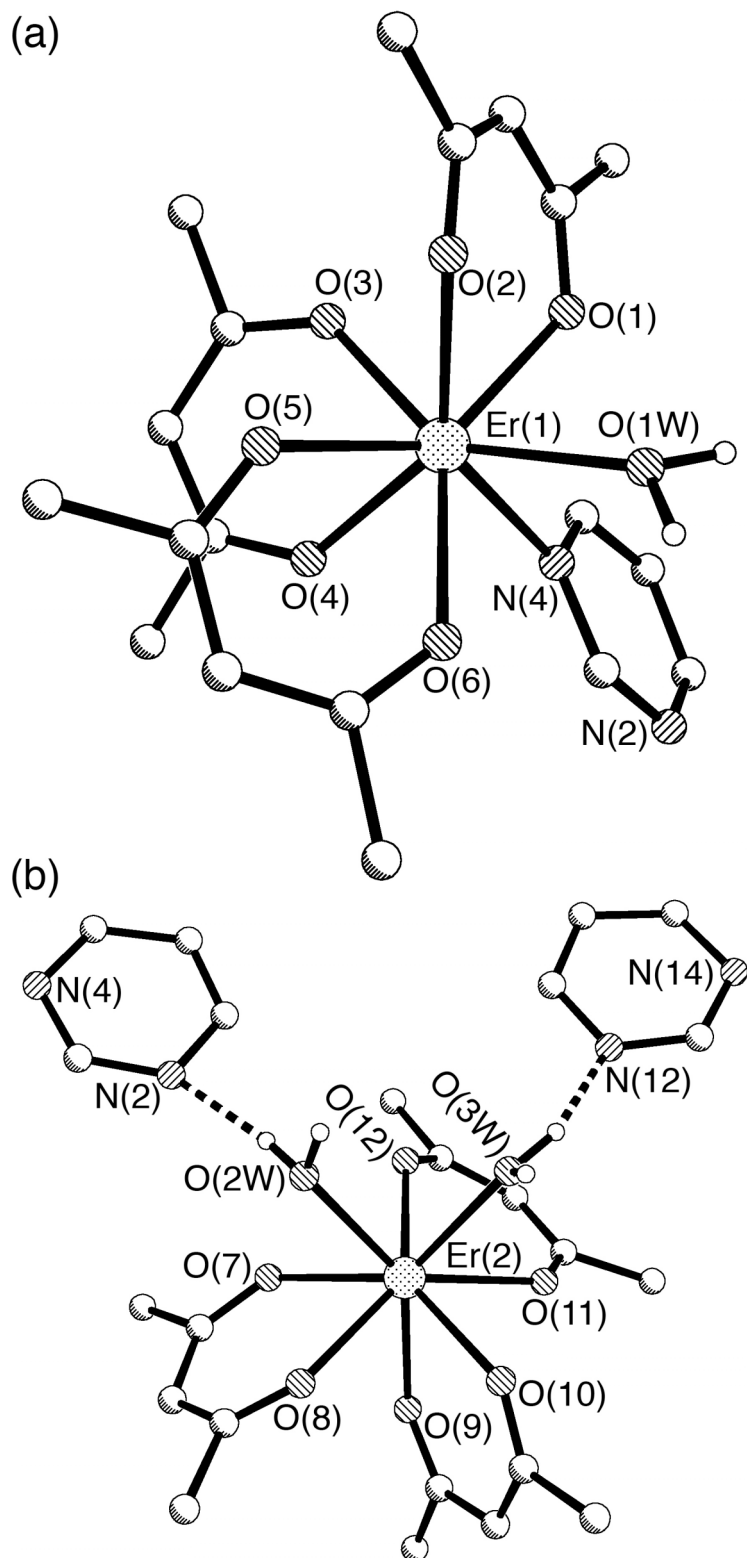


Figure 3

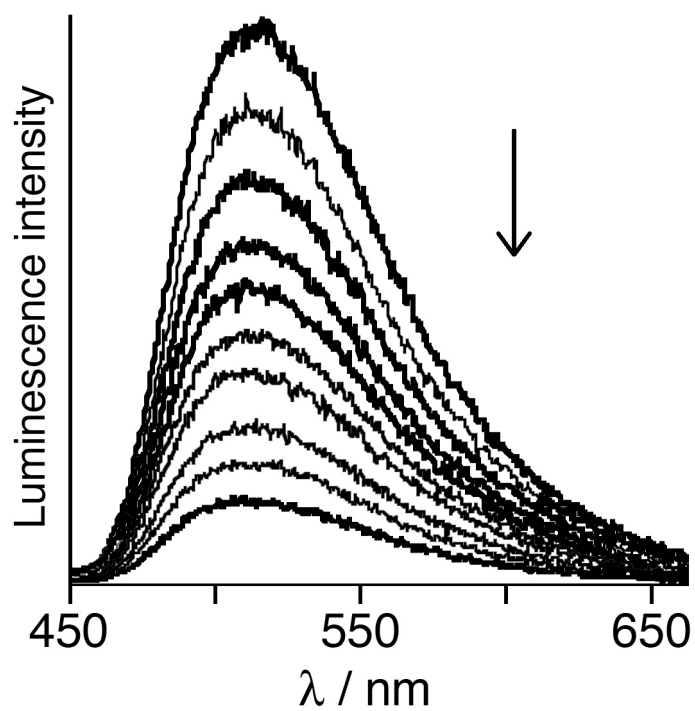


Figure 4

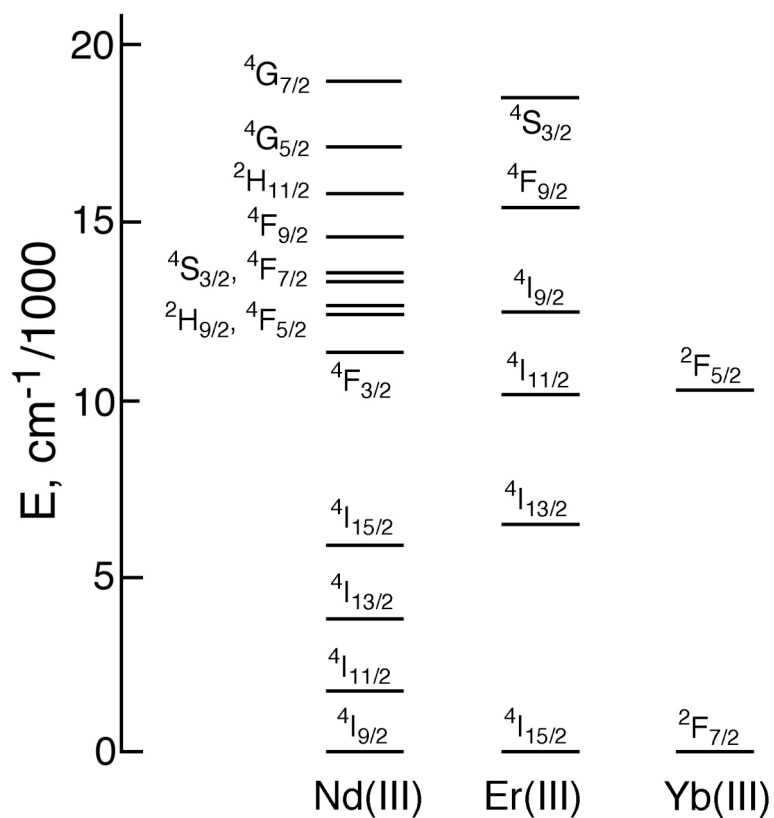


Figure 5

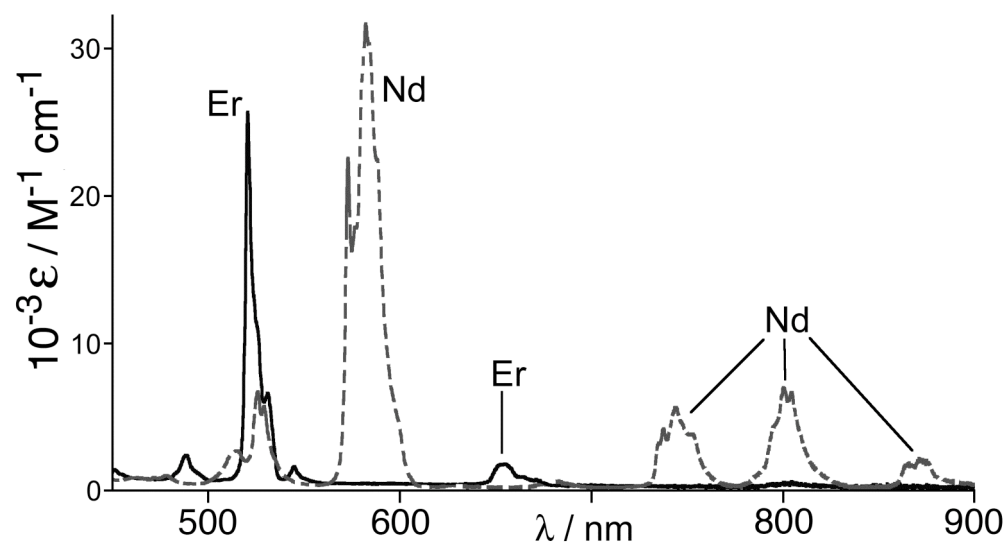


Figure 6

